

CAPACITIVE DEIONIZATION PROCESS WITH DECOUPLED CHARGING AND DISCHARGING FLOW SCHEMES

Ishan Barman[#], Taesik Lee[§], Gyunyoung Heo[†] and Nam P. Suh[§]

Park Center for Complex Systems, Massachusetts Institute of Technology, 77 Massachusetts Avenue, Cambridge, MA 02139, USA

[#]Current address: G. R. Harrison Spectroscopy Laboratory, Massachusetts Institute of Technology, 77 Massachusetts Avenue, Cambridge MA 02139, USA

[†]Current address: Kyung Hee University, 1 Seocheon-dong, Giheung-gu, Yongin-si, Gyeonggi-do, 446-701, Republic of Korea

[§]Current address: Korea Advanced Institute of Science and Technology (KAIST), 335 Gwahangno, Yuseong-gu, Daejeon 305-701, Republic of Korea

ABSTRACT

Cost-effective desalination of saline water, which is more energy efficient than the widely used reverse osmosis (RO) and evaporation processes, is desired to solve the growing freshwater crisis. In recent years, capacitive deionization (CDI), which is based on the principle of electrosorption of ions on charged high surface-area electrodes, has been reported as a promising technology for desalting brackish water, because of its low power requirements. Despite its intrinsic advantages, the low water recovery ratio of CDI, limited plant efficiency and throughput has hindered its development into an industrial process. These problems are a direct consequence of the coupling that exists between the charging and discharging processes. There exist three primary functional requirements for the complete CDI process whereas only two top-level design parameters are utilized to address these.

Using axiomatic design principles, we propose a novel capacitive deionization process employing permeating flow discharge (PFD), which adds a new design parameter (solvent drag) thereby decoupling the functional requirements. In the proposed scheme, waste water is permeated *through* the porous electrodes during the discharging process in contrast to the flow *in-between* the electrodes employed for the AFD process. The underlying principle is that the rate of removal of ions by solvent drag in PFD is significantly greater than by convection-diffusion in AFD. Using a bench-top CDI module, we show that the proposed solution removes the unavoidable coupling present in the AFD scheme. Furthermore we demonstrate a reduction in the discharge time by a factor of two resulting in an approximately 30% increase in the throughput of the CDI process.

Keywords: desalination, capacitive deionization, axiomatic design, electrochemical purification.

1 INTRODUCTION

The presence of water is central to the functioning of all living organisms. The human body consists of approximately seventy-five percent water showing the importance of this single component in the sustenance of life forms. In addition, the importance of water for agricultural and industrial uses – for example, in the form of coolant, reactant and solvent – cannot be overstated. In order to satisfactorily perform most

of the aforementioned functions, it is critical that the solute concentration of the water consumed lies within a specific window of tolerance, as required for the particular process. For example, the physics of the osmosis process necessitates that the fluids used to replenish the body must be less concentrated than the body fluids. The most important consequence of the limitations imposed on the water intake concentration is that seawater and brackish water cannot be directly used, especially for human consumption.

The inadequacy of global fresh water supplies, however, has meant that the quantity and quality of consumable water has sharply declined over the years. The World Water Development Report 2003 [1] delivers the grim prognosis that by the middle of this century, more than 50 nations, constituting a population of about 5 billion, will face a water crisis. The numbers predict a bleak future for a water-stressed society, which increasingly has greater demands for demineralized water and lesser supply avenues to satisfy those demands from. To correct this widening disparity, desalination stands out as an attractive proposition as it can exploit the earth's abundant reserves of saline water in the oceans and seas to generate freshwater suitable for human consumption as well for agricultural and industrial use. Currently, about 12,300 desalination plants world-wide strive to fulfill the objective of treating sea water to make it fit for various applications, primarily human consumption [2]. However, their cumulative contribution is only about 0.3% of the world's water use. While the desalination technology roadmap projects that by 2020 water purification and desalination technologies will contribute significantly to meeting the need to assure a safe, sustainable, affordable and adequate water supply, the current state of the art does not allow desalination to be extensively used. The prohibitive costs associated with the prevailing thermal and membrane-based desalination technologies heavily discourage potential users. Specifically, evaporation and distillation based processes have enormous energy requirements while reverse osmosis-based processes must employ high-pressure pumps to force water against adverse osmotic pressure gradients.

In recent years, capacitive deionization (CDI) has been reported to potentially solve some of the crucial issues that have plagued the existing desalination processes such as energy cost and membrane fouling (see Oren [3] for a comprehensive review on the CDI process). The basic CDI

scheme consists of flow of saline water through a pair of high surface area electrodes (e.g. activated carbon cloth) across which a small voltage is applied. During the flow the ions in the saline water move towards one of the electrodes depending upon the polarity of the ions. The charged porous electrodes are able to electrostatically adsorb the ions in a reversible manner. As a result, during the charging process, capacitive current flows in the external circuit connecting the electrodes and the water flowing out of the system is deionized. Once the capacitor is fully charged, the ions are regenerated by shorting the electrodes (or by applying a reverse polarity). The discharge process, thus, consists of the flushing of the ions adsorbed during the charging process by means of waste water through the same flow path [4].

Although the capacitive process has shown a lot of promise over the last decade or so, it is yet to be fully implemented in an industrial setup. One of the reasons that affect its suitability in such an environment is the low water recovery ratio (with respect to other processes used for brackish water desalination), where water recovery ratio is defined as the ratio of the amount of desalinated water obtained to the total amount of input water. Specifically for the CDI process, the water recovery ratio can be thought as the ratio of the charging time to the time for a complete cycle (charging and discharging), if the flow rates during the cycle are kept constant. For a given throughput of a desalination plant/process, the water recovery ratio and the power consumption per unit volume of water desalinated provide the two most significant metrics for judging the effectiveness of the plant/process. The costs of pumping and pre- and post-treatment of water added to the rising costs of surface water makes maximizing the recovery ratio a priority. In the CDI process, it is observed that the discharge typically takes at least half the time required for charging thereby enabling a maximum recovery ratio of 0.5 – 0.6 (for brackish water desalination) [5, 6]. The corresponding recovery ratios for the RO and EDR processes for brackish water desalination typically exceed 0.85 – 0.94 [7]. It must be noted that throughput consideration is inter-linked to the concept of water recovery ratio, as for a given amount of input water the water recovery ratio of the process determines the system throughput.

The aforementioned problems are a direct consequence of the design coupling that exists between the charging and discharging processes. There exist three primary functional requirements for the complete CDI process whereas only two top-level design parameters are utilized to address these. In this paper, we propose a novel capacitive deionization process employing permeating flow discharge (PFD) which adds a new design parameter (solvent drag) thereby decoupling the functional requirements. In the proposed scheme, waste water is permeated *through* the porous electrodes during the discharging process in contrast to the flow *in-between* the electrodes employed for the AFD process. The underlying principle is that the rate of removal of ions by solvent drag in PFD is significantly greater than by convection-diffusion in AFD. Using a bench-top CDI module, we show that the proposed solution removes the unavoidable coupling present in the AFD scheme. Furthermore we report that over time scales around the discharging time constant of the effective

circuit, the permeating flow scheme is able to remove twice as many ions from the setup as the AFD technique. This indicates a reduction in the discharge time by a factor of two resulting in an approximately 30% increase in the throughput of the CDI process.

2 PROPOSED DESIGN FOR PERMEATING FLOW DISCHARGE BASED CDI PROCESS

As briefly mentioned in Sec-1, in the capacitive deionization process, the product water is produced only during the charging period of the total cycle. The discharge time enables recharging of the electrodes but the water that flows through the channel during the discharge half cycle cannot be utilized. In this paper, our primary objective is to develop a scheme that can significantly reduce the process downtime (discharge time) while retaining the equivalent functionality of regenerating the electrode.

It should also be mentioned at the outset that in a typical CDI process, the 'transition' phase between the charging and the discharging phases of a cycle and the 'turnaround' phase between the discharging and charging phases of two successive cycles do not contribute to the water throughput for the plant. These time periods need to be factored in for a precise computation of the performance metrics. We will henceforth group these two phases together and call it the switching phase because in essence this is the time that is required to switch between the desalination (charging) and regeneration (discharging) phases.

While the need to reduce the total downtime as well as the amount of water for regeneration has been well-documented [8, 9], the proposed solutions introduce additional regenerant fluids and charge barrier membranes, which introduce new complexities such as substantially higher pressure drops, membrane scaling and fabrication difficulties. Consequently, there is a desperate need for a design solution to reduce the stated downtime, which does not adversely affect the basic functioning of the CDI process.

In developing the CDI process, we are faced with a situation where knowledge of the process itself is inadequate in terms of identifying the critical drawback in the existing design. To identify the said drawback, we employ the axiomatic design methodology [10]. Axiomatic design provides a scientific foundation for design by systematically analyzing customer attributes (CA) and mapping them successively into three generic domains - functional requirements (FR), design parameters (DP) and process variables (PV). By using the two fundamental axioms that govern the decision making process, one can create a rigorous interplay between "what we want to achieve" and "how we plan to achieve it". The main step in axiomatic design is to establish a design matrix between the characteristic vectors that define the design goals and the corresponding solutions. The design matrix at the topmost level consists of a set of Xs and Os to understand the effect of the various design parameters on the functional requirements (where an 'X' indicates significant impact on the FR by the given DP and a 'O' indicates little or no impact on the FR by the corresponding DP). After decomposition of the design matrix, which is performed by zigzagging between the FR and DP domains, further design details can be incorporated. For the

CDI process, we will only be concerned with the design intent and thus subsequent decomposition will not be necessary.

The first step in formulating the FR-DP mapping is to identify the multiple FR. These are the highest level functions which the process/system has been designed to satisfy. To establish a clear set of FRs, we need to understand the physical processes that drive the deionisation process. The CDI process is based on a physicochemical reaction, which takes place only in a restricted region, i.e. on the surface of the carbon aerogel electrodes. A reaction of this kind is commonly termed as a heterogeneous reaction, as opposed to a homogeneous reaction where the reaction takes place in the bulk of the fluid. It should be noted that most of the high surface area electrodes, including carbon aerogel, are fairly porous and the ions adsorbed in the electrical double layer (EDL) not only appear in the flat surface region but also in the interior where they are adsorbed to the EDL of the inner particle clusters or fibers. The EDL is typically considered to occur within a few nanometers of the actual charged layer.

The heterogeneous reaction under consideration here consists of three primary steps. The first step involves the transport of the reacting species (ions) to the electrode surface (carbon aerogel). In this step, the presence of electric field is significantly more important than lateral diffusion for migration of ions to the electrode. The (axial) convection process is responsible for bringing more ions into the system. The second step entails a series of substeps including diffusion of ions through the aerogel, adsorption on the surface, subsequent desorption, and diffusion of ions through and out of the surface. The third step is a direct reversal of the first step and deals with the transfer of ions away from the reaction surface and its neighbourhood into the bulk phase. This description of the phenomenon is fairly generic and is typically applied to chemically catalyzed reactions at solid surfaces, enzyme-substrate reactions at interfaces and electrode reactions in electrochemical cells. The second step is the significant step in the actual deionization process but is rate-limited by the transfer phenomena of steps one and three. In this phenomenological depiction, the first half of the second step (i.e., adsorption on the surface) completes the charging portion of the cycle while the latter half of the same step (i.e. desorption of ions from the surface and subsequent diffusion of ions through and out of the surface) initiates the discharging part. Based on this three-step picture, we establish the appropriate FR-DP relations as shown in Eq. (1).

$$\left\{ \begin{array}{l} FR1 : \text{Transport ions from bulk to electrode} \\ FR2 : \text{Adsorb (desorb) ions from electrode} \\ FR3 : \text{Transport ions from electrode to bulk} \end{array} \right\} = \begin{bmatrix} X & X \\ 0 & X \\ X & 0 \end{bmatrix} \left\{ \begin{array}{l} DP1 : \text{Convection - diffusion} \\ DP2 : \text{Electric field} \end{array} \right\} \quad (1)$$

We observe from Eq. (1) that there are only two design parameters at the highest level to satisfy the three top-level functional requirements. In a scenario where the number of FRs exceeds the number of DPs, the design becomes 'coupled'. A coupled design does not satisfy the independence

axiom and consequently successful attainment of design goals becomes an improbable task, if not an impossible one. The capacitive deionization process design involving axial flow discharge is not a desirable solution and one must look to either 'uncouple' or 'decouple' the design. A decoupled design is characterized by a triangular (either upper or lower triangular) design matrix while for an uncoupled design, the design matrix assumes a diagonal form.

Evidently, the uncoupled design is the best possible form since each FR is independently satisfied by its corresponding DP (FR1 by DP1, FR2 by DP2 and so on). However, it is not always possible to attain a simple uncoupled form. In such a scenario, a decoupled design works equally effectively as long as the DPs are implemented in the sequence dictated by the triangular form of the design matrix. The easiest way to decouple the design, presented in Eq. (1), is to either add a DP or reduce a FR. However, the reduction of a FR is an unacceptable practice, as that would mean the reduction of functionality of the system and consequently an inability of the system to attain its desired goals. Thus, our new design should incorporate an additional DP such that the new design is able to satisfy the independence axiom. Loosely speaking, the new DP should significantly influence its corresponding FR while having limited or no impact on the other FRs. It is to be noted that this is not a strict requirement but given multiple possible DPs, one would like to introduce a DP that follows the above norm.

Motivated by this bottleneck in the CDI process, we propose a novel discharge technique that can eliminate the source of coupling in the CDI technique. Such a design should be able to significantly reduce the downtime enabling an increase in water recovery ratio to the levels of the other brackish water desalination processes such as reverse osmosis and EDR. In the proposed discharge scheme, which we call the permeating flow discharge (PFD), the waste water is permeated *through* the porous electrodes (see Fig. 1 below) rather than the conventional flow path of *in-between* the electrodes in the axial flow discharge (AFD) process. This new flow path for the discharge scheme introduces a new DP that can directly address FR3 ("Transport ions from electrode to bulk") while not affecting any other FRs. As this flow path is utilized during the discharging process only, it does not have any influence on FR1 ("Transport ions from bulk to electrode"). Furthermore, FR2 is restricted to the involvement of electrochemical phenomena only (and is independent of any ion transport process), i.e. adsorption and desorption of ions from the high surface area electrodes – and is thus not affected by the introduction of the new DP.

The permeation flow is controlled by either forcing a fixed amount of fluid through the porous electrodes or by maintaining a given pressure differential across the middle and outer channels. In the latter case, the pressure differential modulates the permeation flow velocity. It should be noted that the permeation flow velocity depends on the material properties of the porous electrode, especially its overall porosity.

The new DP introduced by permeation of the waste water through the porous electrodes is called solvent drag. It represents the phenomena of ion transport through a membrane (the porous electrode in this case) due to constant

solvent flux through the same. In other words, the solute is carried with the solvent as the latter perfuses through the carbon aerogel electrodes. It must be emphasized that the solvent drag phenomena is completely distinct from the diffusion of the ions across the porous electrode due to the concentration difference that exists across it. The solvent drag term and the diffusion term together account for all of the ions transported across the aerogel electrode. The new FR-DP mapping based on the deionization process employing the PFD scheme is shown in Eq. (2).

$$\left\{ \begin{array}{l} FR1 : \text{Transport ions from bulk to electrode} \\ FR2 : \text{Adsorb (desorb) ions from electrode} \\ FR3 : \text{Transport ions from electrode to bulk} \end{array} \right\} = \left\{ \begin{array}{l} DP1 : \text{Convection - diffusion} \\ DP2 : \text{Electric field} \\ DP3 : \text{Solvent drag} \end{array} \right\} \quad (2)$$

The relative magnitude of the solvent drag, diffusion-across-membrane and internal diffusion terms - where the first two regulate the PFD ion transfer phenomena and the last term accounts for ion transport in the AFD scheme - will determine the effectiveness of the new process. Although it is not imperative to have solvent drag to be substantially higher than diffusive permeation across the aerogel electrode, one would expect this to be the case unless the permeation velocity is extremely small. This reasoning forms the basis of the smaller 'x' (denoting smaller influence) in the 1st column of the 3rd row as compared to the larger 'X' (depicting significant influence) in the 3rd column of the same row. It is to be noted that even if this were not true, the design matrix would still be decoupled.

What is of far greater consequence, however, is the ratio of the sum of the PFD ion transfer terms to the AFD ion transfer term. For maximum benefit, the former should be substantially higher than the latter. In other words, the new scheme will be able to cause a significant change in the performance metrics of the CDI process if and only if the ions that are desorbed from the aerogel electrode are removed much faster with the help of the permeation flow path. The understanding that the ion removal rate is inherently linked to the performance metrics, primarily water recovery ratio and throughput, gives rise to the underlying hypothesis of our work, which can be formally stated in the following manner:

The rate of removal of ions from a channel setup is higher for a process that is influenced by solvent drag (PFD) than for one which is diffusion limited (AFD), given the same flow conditions.

3 MATERIALS AND METHODS

A multi-channel experimental setup was designed to test the aforementioned hypothesis and to determine the extent of benefit obtained by employing one flow scheme with reference to the other. A schematic of the implementation of the two processes – AFD and PFD - is shown in Fig. 1. It is to be noted that Fig. 1 depicts the discharging flow paths only.

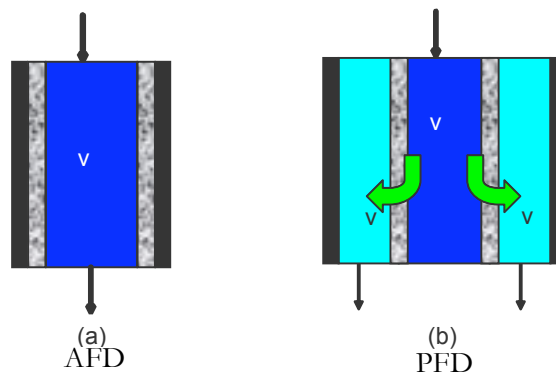


Fig. 1: Schematic diagram of the AFD and PFD schemes. The flow paths shown are applicable for the discharging phase only.

To fabricate the multi-channel setup, the channel frames were first machined from polypropylene sheets, having a thickness of 8 mm. The channel frames provided the space for the water chambers, each of which was 23 cm long and 7 cm high (Fig. 2). Evidently, the width of the chambers was the same as the thickness of the frames, i.e. 8 mm. Two holes were drilled in each frame to facilitate for tubing connections from the pump to the input side and from the outlet to flow control valves. The central channel was enclosed by carbon aerogel papers (0.25 mm thick), which formed the high surface area porous electrodes. Aluminum foils, which were directly connected to the external electrical circuit, were put in direct contact with the carbon aerogel papers. Care was taken to ensure that the contact resistance between the conductive foil and the aerogel paper was negligible by applying adequate pressure on the outermost retainer plates.

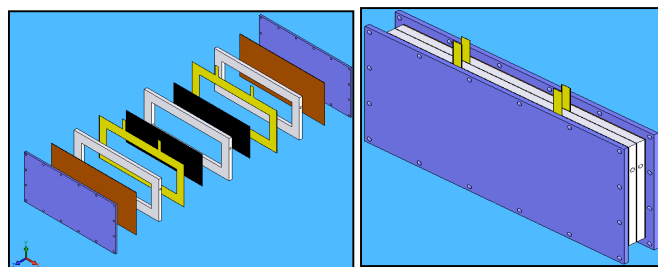


Fig. 2: CAD model of the three channel setup (exploded view – left; isometric view - right): polypropylene sheets (purple); rubber gasket (brown); polypropylene channel frames (white); aluminum foil (yellow); carbon aerogel sheets (black).

Extensive research has gone in to the design and fabrication of high surface area materials, primarily for the development of supercapacitors and capacitive deionization systems. Specifically, the introduction of carbon aerogel as a high surface area electrode material can be said to have provided the mainspring for widespread interest in the development of capacitive deionization systems. Due to the intrinsic advantages of high surface area, low resistance and high relative capacitance, carbon aerogel sheets were chosen for the capacitive electrodes used in this study. It is to be noted that carbon aerogel, which is manufactured by pyrolyzing carbon fibers impregnated with resorcinol-formaldehyde aerogel, displays typical porosity values of 50-

80%, due to the cumulative contribution of the embedded mesopores and micropores. The carbon aerogel sheets used in this study, RF paper (MarkeTech International Inc., Port Townsend, WA), have the following specifications: density of 0.4-0.5 g/cc; surface area of 400-500 m²/g; capacitance of 15-19 F/g and specific electrical resistivity of 0.01-0.04 Ω-cm.

To demonstrate the validity of the hypothesis stated in Sec-2, the assembled setup was employed in two full operational cycles multiple times, where one operational cycle consists of charging, transition, discharging and turn-around phases. Evidently, the discharging phase is of primary importance in terms of the hypothesis – the rest of the phases remain invariant during AFD and PFD cycles. To start the charging process, saline water was pumped into the channels. During the charging period, water was allowed to stand still inside the setup rather than flow through it. The primary motivation in letting no flow occur during the charging phase was to obtain sufficient desalination (concentration difference between the input and the output streams), given the limited functional area of the electrodes. The bench-top setup in our experiment used carbon aerogel electrodes, each having a flat surface area of 161 cm². Typically, one would need much larger areas (longer/wider channels) to obtain adequate desalination in the flow mode. Given the dimensions of our setup, in the continuous flow condition, even after saturating the electrodes, we might not have been able to detect a significant concentration difference due to the fact that the same number of ions would have been removed from a substantially larger volume of water. While this operation does not truly simulate that of an industrial plant, it helps us make accurate predictions about the system throughput and water recovery ratio and provides valuable insight into the nature of scaling required for a viable commercial setup.

In the no-flow state, the setup, for both AFD and PFD experiments, was charged till the potential difference across the electrodes reached a pre-fixed value, which for our experiments was assigned to be 430 mV. It is important to mention that the battery connected for charging must have a potential difference less than 1.3V to ensure that the water in the channels does not ionize. After the completion of the charging phase, the contents of the channels were emptied (transition phase) and the final concentration of the deionized water was measured by a TDS meter (TDS4, Industrial Test Systems, Inc., SC). Since the TDS meter used was most sensitive in the 1-999 ppm (parts per million) range with a resolution of 1 ppm, the concentration of the input stream (produced by mixing deionized water and table salt) was varied between 600 and 900 ppm. The mass of ions removed during the charging phase was then calculated by using the concentration value of the saline water input to the system and that of the final outlet stream. The measured charging current provides an additional check on the calculation of the deionized mass value.

After the charging and transition phases were completed, the electrodes were shorted and the discharging flow paths for the AFD and PFD cycles were implemented. To implement the two separate flow schemes, we used a fluidic circuit consisting of a pair of peristaltic pumps, in conjunction with flow control valves, to maintain a specified flow rate between

a pair of adjoining channels. The two peristaltic (positive displacement) pumps (43045K36, McMaster-Carr, CA), which were employed to feed water at flow rates ranging from 7 ml/min to 207 ml/min, were connected to the middle channel and the outer channels. The experiments were performed at permeation flow rates of 0 (AFD case), 8, 16, 32 and 64 ml/min respectively. The pump was able to handle a maximum pressure of 20 psi (138 kPa), which was sufficient as the maximum pumping requirement for the current setup was only 6 psi (41 kPa).

For the AFD flow case, no pressure difference was maintained across a pair of channels to ensure that the flow was *in-between* the electrodes, similar to that employed during the charging cycle. The PFD experiments were performed in two different ways: (a) by closing the central channel valve and the pump connected to the outer channels, such that all the water input into the central channel was forced to permeate through the porous electrodes into the outer channels; and (b) by operating the pump connected to the central channel at a higher flow rate than that connected to the outer channels, where the difference in flow rate is equal to the designed permeation flow rate across the electrodes. The permeated water, after moving through the aerogel electrodes and the outer channels, was collected in a beaker. The two outer channel outlet streams were collected together and the combined volume flow rate was identical to the flow rate of the outlet stream in the AFD setup. The outlet concentrations, for both AFD and PFD experiments, were measured at definite time intervals. The experiments were carried out till the discharging current fell to less than 5% of its initial value. The input water used for our discharging processes was tap water (~300 ppm). This ensured that the collected water never crossed the 999ppm mark, as required by the TDS meter, even after carrying the ions from the channel or through the electrode.

The measured discharging current also provided an estimate of the number of ions that had been detached from the electrodes. In essence, this could be thought of as the upper bound to the cumulative mass of ions removed because the transfer of ions from the surface to the bulk (where bulk could mean either the middle channel or the outer channels) is preceded by the dissociation reaction at the surface (desorption).

4 RESULTS AND DISCUSSION

4.1 CHARGING PROCESS

In this section, we derive an analytical expression for the amount of time a system can be charged before it needs to be regenerated, i.e. the permissible charging time per cycle. In order to do so, we must have knowledge of the following parameters to calculate the permissible charging time period for the CDI process:

- The permissible level of concentration in the output (product) water (c_{perm} ppm),
- Flow rate of water in the system (Q ml/min),
- Time constant for charging the capacitor (τ sec),
- Initial value of the charging current (I_0 A).

The first parameter, the tolerable level of concentration in the product water, is specified by the end user. Naturally, for higher permissible levels of output concentration, the

charging can take place for a longer period. The second parameter (flow rate) is a system parameter. In ideal conditions, we would like our system to have as high a flow rate as possible to ensure maximum throughput. However, higher flow rates would mean the ions are being pushed through the channel at a faster rate and are getting much less time during which they can be attracted and adsorbed on the electrodes. As a consequence, more number of ions will tend to remain in the product water.

The final two parameters (c) and (d) stated above pertain to the variation in the charging current with time. We assume that the current in the charging phase exhibits a mono-exponential decay profile and thus only these two parameters, the initial value and the time constant, are sufficient to determine its value at any point of time. Our experiments show that the exponentially decaying profile provides an excellent approximation to the actual charging current characteristics. The mathematical expression for the permissible charging cycle time can be derived in the following manner:

$$\text{Rate of removal of ions at any time } t = \frac{I(t)}{F}, \quad (3)$$

where $I(t)$ is the current at that time instant and F is the Faraday constant (96,485.3383 C/mole).

Given that the flow rate in the system is Q ml/min,

$$\text{reduction in concentration } (\Delta c)_t \text{ at time } t = \frac{60 I(t)}{F Q} \text{ moles/ml} \quad (4)$$

Converting this value to a ppm (mg/l) concentration, we have:

$$(\Delta c)_t = 60 \cdot 10^6 \frac{M I(t)}{F Q}, \quad (5)$$

where M is the molecular weight of the salt (for NaCl, $M = 58.442$ g/mol).

It is evident that $(\Delta c)_t$ is the critical parameter in making the decision when charging must end, because if $(\Delta c)_t$ falls below a minimum threshold value, the product water concentration will cross the permissible levels. The threshold value for the desalination required is given by:

$$(\Delta c)_{\text{threshold}} = c_{\text{input}} - c_{\text{perm}}, \quad (6)$$

where c_{input} is the concentration of the input water in ppm.

Since, $(\Delta c)_t$ must be greater than or equal to $(\Delta c)_{\text{threshold}}$, we can write from Eq. (5) and (6):

$$c_{\text{input}} - c_{\text{perm}} \leq 60 \cdot 10^6 \frac{M I(t)}{F Q}. \quad (7)$$

Substituting for $I(t)$ the exponential decay profile, given the initial charging current (I_0) and the charging time constant (τ), we get:

$$c_{\text{input}} - c_{\text{perm}} \leq 60 \cdot 10^6 \frac{M I_0}{F Q} \exp\left(-\frac{t}{\tau}\right). \quad (8)$$

Simplifying the above expression in the limiting case and putting M equal to 58.442 g/mol, we have:

$$t_{\text{critical}} = \tau \left[10.5 - \ln\left(\frac{Q \cdot (c_{\text{input}} - c_{\text{perm}})}{I_0}\right) \right], \quad (9)$$

where t_{critical} is the maximum time for which the charging phase can be continued in one cycle.

As stated in Sec – 3, the charging experiments were performed in the no-flow state so as to enable us to obtain the maximum possible desalination for the volume of water pumped into the channel before the start of the charging phase. Given the no-flow constraint, the main sources of meaningful information are the current characteristics obtained as a function of time during the charging cycle. The current curves obtained closely follow the classical exponential profile associated with charging of capacitors with the following characteristic constants: $I_0 = 19.6$ mA and $\tau = 14.16$ min. We also measured the difference in concentration before and after the charging cycle for the saline feed into the setup. The measured concentration difference for the water had a mean value of 35 ppm, with a standard deviation of 8 ppm. Furthermore, one can also compute this concentration difference by determining the mass of ions removed from the current characteristic curves. It is found that the calculations based on the current curves predict a concentration difference of 35.8 ppm between the inlet and the outlet streams, given that the setups deionised a total volume of 160 ml. The experimentally measured concentration difference, therefore, shows excellent correspondence to the theoretically predicted concentration difference based on the charging current characteristic curves.

Although the above calculations for the concentration difference obtained provide us with a reference point for the deionization process, it does not provide any insight for the computation of the performance metrics, i.e. water recovery ratio and throughput. The key step towards quantification of these two metrics is the determination of the permissible charging time value, as given by Eq. (9). Fig. 3 shows the plot of permissible charging time (t_{critical}) versus flow rate (Q), obtained using Eq. (9), for different values of permissible output concentrations (c_{perm}):

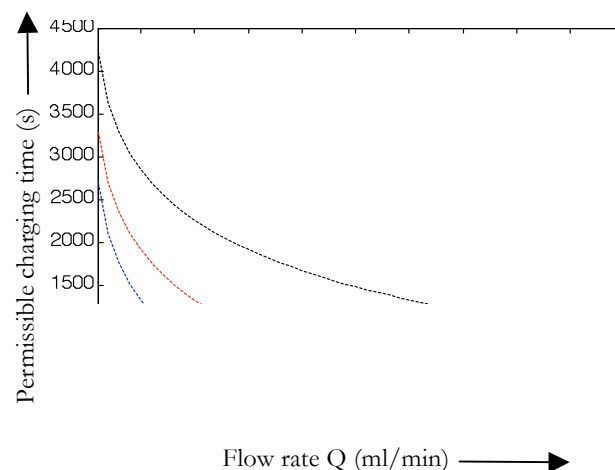


Fig. 3: Plot of permissible charging time versus flow rate for different values of permissible output concentration. The blue line, red line and black lines map the expected charging times for c_{perm} equal to 30 ppm, 15 ppm, and 5 ppm below the input concentration respectively. Charging current parameters employed for this simulation: $I_0 = 19.6$ mA and $\tau = 14.16$ min.

4.2 DISCHARGING PROCESS

The discharging cycle observations are analyzed in this section to test the hypothesis presented in Sec-2. Additionally, these results, in conjunction with the observations of Sec-4.1, enable us to compute the performance metrics of the CDI process employing the AFD and PFD schemes, respectively.

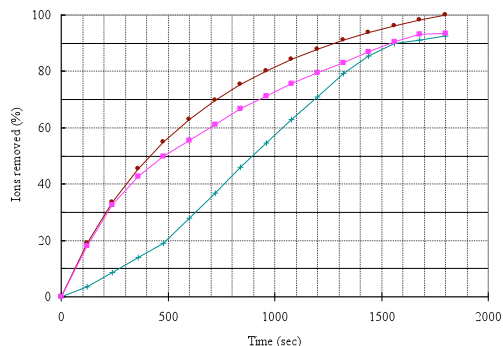


Fig. 4: Plot of percentage ion removal as a function of time for the AFD (cyan) and PFD (magenta) process for flow rate of 16 ml/min. The topmost curve (brown) quantifies the percentage of ions detached from the electrical double layer of the capacitive electrodes over the same time duration.

Fig. 4 plots the percentage of ions removed as a function of time using the AFD and PFD schemes (for system flow rate of 16 ml/min). Here, the topmost curve, which is obtained from the experimental current calculations, represents the strict upper bound to the process, given the two-step heterogeneous reaction for the desorption and discharge from the system. The percentage of ions removed was calculated by converting the ratio of the mass of ions removed at any instant of time to the total mass of ions detached from the paper in three time constants to a percentage value. The striking feature of Fig. 4 is the distinctiveness of the AFD and PFD profiles for the ion removal rate. It can be observed that over time scales in the range of 400-800 seconds, there is a significant difference in the ion removal capability of the two processes (the time constant of the discharging processes was measured to be 550 seconds). Over time scales significantly longer than that mentioned above, the two mass transfer processes tend to remove ions from the system with equal efficiency. It should be noted that in three time constants a capacitor should discharge about 95 percent of its accumulated charges.

For the AFD case, the observed profile follows the expected S-shape as the primary phenomenon driving the AFD process is convection-diffusion. Typically, this kind of profile is associated with any mass transfer process that has any diffusive characteristics. The initial progress is fairly slow because the diffusion phenomenon needs a certain amount of time (sometimes called the time lag) to transfer the detached ions from the surface of the porous electrode to the bulk of the channel. In addition, the axial flow velocity is maximum at the channel center and zero at the electrode surfaces. As a result, the convection process cannot flush out the ions till the diffusion process transfers the ions from the electrode surface towards the bulk of the channel system. Furthermore, the initial concentration of detached ions at the aerogel surface is

not very high, which means that there exists only a limited concentration gradient to drive the diffusion process. Subsequently, however, the electrode surface concentration rapidly picks up creating a sufficiently high concentration gradient in the lateral direction. As a consequence, the process speeds up on time scales longer than the lag time, and the convective flow is able to carry away the ions that have moved away from the electrode surface by lateral diffusion. On even longer time scales, after about 1400 seconds as observed from Fig. 4, the process slows down as most of the detached ions have already been removed. The discharging current has dropped down appreciably by this point of time thereby releasing lesser number of detached ions into the flow channel.

For the PFD process, on the other hand, no characteristic lag can be observed in the experimental plot. The permeating flow discharge process removes the ions through the porous electrodes in two different ways: (a) the first contribution comes from the solvent drag term, where the amount of ion removal is directly proportional to the concentration on the electrode surface as per the modified Kedem-Katchalsky equation [11] and (b) the second contribution is from the diffusive flux that arises due to the concentration difference across the electrodes. The lack of the characteristic lag time is because both the solvent drag and diffusion across the electrode respond to the build-up of concentration at the electrode surface. The profile here mirrors the plot of cumulative ions detached from the EDL of the aerogel electrode versus time. Depending on the concentration at the electrode, the solvent is able to drag a proportional number of ions along with the flow. In this case, the highest removal rate occurs when the concentration at the electrode is maximum, i.e. when the discharging current has reached its highest value (more precisely, the removal rate is maximum when the cumulative build-up of ions at the electrode is the highest). Moreover, once the electrode has been crossed the ion can be considered to be removed from the system, which is in sharp contrast to the AFD process where the lateral diffusion provides an intermediate pathway before the ion is finally flushed out by the convective flow. It is to be noted that the solvent drag term is much more effective as it is proportional to the concentration at the electrode surface unlike the diffusive flux term which varies linearly with the difference in concentration between the two channels across the electrode surface.

From Fig. 4, it is evident that the performance of PFD in removing ions from the CDI system is significantly better than AFD on time scales close to the time constant of the discharging circuit. Based on the previous discussions of the physical processes that drive the different flow schemes, this behavior is expected as the PFD process is fast enough to remove the ions detached during the shorter time scales. This validates the hypothesis of Sec-2, that the permeation flow scheme is able to remove ions at a much faster rate than the existing axial flow discharge schemes, under the same flow conditions. For example, the PFD and AFD processes require 500 and 900 seconds, respectively, to remove 50% of the ions from the system – a reduction of nearly a factor of two in discharging time. On longer time scales, however, due to the fall of the discharging current and the speeding up of the

convection-diffusion phenomenon the significant advantage of PFD over AFD reduces.

The above experimental observations reveal that the performance metrics of the CDI system is intrinsically correlated to the percent of ion removal from the system in each cycle, primarily because of the fact that the discharge time varies as a function of percentage of ion removal from the system. Thus there is a need to formulate the performance metrics, i.e. water recovery ratio and throughput, as functions of discharge percentages. It is to be noted that a lower discharge percentage means that the charging process is able to only partially utilize the aerogel paper, e.g. if we only discharge up to 50% of the total ions, the charging can take place from 50% to the point where the current falls below the threshold level, indicative of insufficient deionization from the system. Nevertheless, if the water recovery ratio per cycle increases substantially, the net effect of the increased water recovery ratio and number of cycles will more than compensate for the reduction of throughput per cycle.

For the example of 50% discharging time mentioned in the above paragraphs, Eq. (9) yields that the charging time, for a flow rate of 16 ml/min and a 15ppm difference between the input and the acceptable output concentrations, is equal to approximately 350 seconds. The time required for the corresponding discharge cycles is 500 and 900 seconds for the PFD and AFD processes (also at 16 ml/min), respectively. To a first order approximation if we neglect the time necessary for switching (transition and turnaround phases), we observe that the water recovery ratio for the PFD case is approximately 30% better than that obtained on employing the AFD process. It is to be noted that these parameters are not optimized for water recovery ratio and throughput but provide an indication of the extent of benefit that can be obtained by employing the PFD process. A detailed investigation of the performance metrics for the two processes (AFD and PFD), along with the theoretical predictions of the optimal flow rate, will be addressed in a future publication.

5 CONCLUSION

Desalination provides a technological solution to overcome the increasing barriers of water scarcity by desalinating the abundant reserves of seawater and brackish water. The existing desalination technologies, unfortunately, are unable to fill the space, primarily due the prohibitive energy costs associated with these processes. Over the last decade, the capacitive deionization technique has been earmarked as a promising approach to deionise saline water. However, this technique, while enjoying almost an order-of-magnitude advantage in terms of energy costs, is plagued by its poor water recovery ratio and limited throughput characteristics. These problems are a direct consequence of the coupling that exists between the charging and discharging processes. There exist three primary functional requirements for the complete CDI process whereas only two top-level design parameters are utilized to address these.

In this paper, we use axiomatic design principles to propose a new discharge methodology, which can significantly raise the water recovery ratio and throughput of the capacitive deionization technology. The underlying hypothesis of this

discharge technique, which we call the permeating flow discharge scheme, is that the ions detached from the electrical double layer of the capacitive electrodes are removed at a faster rate by flow through the electrodes than by the conventional axial flow in between the electrodes. Based on the physical phenomena that determine the two discharge methods, namely solvent drag and internal diffusion, it is shown that the permeating flow discharge scheme is able to decouple the intrinsically coupled CDI process.

Using a bench-top experimental setup, we have demonstrated that over time scales in the range of the discharge circuit time constant, the permeating flow scheme is able to remove twice as many ions from the setup as the conventional axial flow technique. This implies a similar reduction in the discharge time, for reduced discharge percent cycles, resulting in an approximately 30% increase in the throughput of the CDI process.

Further work in consolidating this approach will involve the development of a scaled-up facility to test the predictions for power consumption, water recovery ratio and throughput. Additionally, this facility will be able to determine the long-term operational effectiveness of the CDI process employing the permeating flow discharge scheme. The fabrication of supercapacitor materials, having significantly higher surface area than the existing carbon aerogel sheets, would also greatly aid in establishing this technology on an industrial scale.

6 REFERENCES

- [1] "Water for people, Water for life", World Water Development Report, United Nations, 2003.
- [2] "The 19th IDA Worldwide Desalting Plant Inventory", Global Water Intelligence, Aug 2006.
- [3] Oren, Y., "Capacitive deionization (CDI) for desalination and water treatment – past, present and future (a review)", *Desalination* 228, pp. 10-29, 2008.
- [4] Farmer J. C., "Method and apparatus for capacitive deionization and electrochemical purification and regeneration of electrodes", *U.S. Patent* No. 5,954,937, 1999.
- [5] Welgemoed T. J., Schutte C. F., "Capacitive desalination technology: an alternative desalination solution", *Desalination* 183, pp. 323- 340, 2005.
- [6] Lee J-B., Park K-K., Eum H-M., Lee C-W., "Desalination of a thermal power plant wastewater by membrane capacitive deionization", *Desalination* 196, pp. 125-134, 2006.
- [7] Allison, R. P., "High water recovery with electrodialysis reversal," *Proceedings American Water Works Assoc. Membrane Conference*, Baltimore, Aug. 1-4, 1993.
- [8] Tran T. D., Farmer J. C., Murguia L., "Method and apparatus for capacitive deionization and electrochemical purification and regeneration of electrodes", *U.S. Patent* No. 6,309,532, 2001.
- [9] Andelman M. D., Walker G. S., "Charge barrier flow-through capacitor", *U.S. Patent* No. 6,709,560, 2004.
- [10] Suh N.P., *Axiomatic Design: Advances and Applications*, Oxford University Press, 2001. ISBN 0-19-513466-4
- [11] Kedem O., Katchalsky A., "Thermodynamic analysis of the permeability of biological membranes to non-electrolytes", *Biochimica et Biophysica Acta*, Vol. 27 (229), pp. 413-430, 1958.